JOURNAL OF OPTOELECTRONICS AND ADVANCED MATERIALS, Vol. 10, No. 10, November 2008, p. 3150 - 3157

Influence of the excitation voltage on the electroluminescence of PVK-based Polymer Light Emitting Diodes with different electrochemically-deposited PANI buffer layers

J. L. ALONSO*, J. C. FERRER, S. FERNÁNDEZ DE ÁVILA
Dpto. de Física y Arquitectura de Computadores, Universidad Miguel Hernández, Av. de la Universidad s/n, Ed. Torrepinet, 03202, Elche, Alicante, Spain

Polymeric light emitting diodes based on *Poly(9-vinylcarbazole)* have been fabricated. Electrochemically deposited polyaniline (PANI) films of several thicknesses have been used onto the ITO-covered glass substrates as buffer layers. An experimental study about the dependence of the Electroluminescence on the excitation voltage of these devices with different thicknesses of PANI buffer layers has been carried out. A comparison has been established with devices with PEDOT:PSS buffer or without any buffer layer. A lower turn-on voltage has been found for devices using thicker PANI buffer layer. Electroluminescence measurements suggest that the energy emitted varies exponentially with the excitation voltage of the devices. A demonstration has been done by calculating the area under the electroluminescence curves and fitting the results as a function of the excitation voltage.

(Received April 10, 2008; accepted October 30, 2008)

Keywords: Polymeric light-emitting diodes, Polyaniline, Hole-transporting layers, Electrochemically-deposited, Spin-coating, Electroluminescence

1. Introduction

Since the first successful demonstration of polymer light emitting diodes (PLEDs) [1-3] from a conjugated polymer in 1990, PLEDs have attracted worldwide attention as candidates for the next generation of emissive flat panel displays, and the same organic structures have been used as light detector devices like photodiodes or solar cells [4-8].

The wide experience reached in the development of inorganic semiconductor based optoelectronics has allowed a fast progress in this field. Furthermore, the advantages shown by these polymer LEDs in contrast to inorganic ones rest on the ability of depositing thin polymer films using low cost methods like spin-coating, ink-jet printing, etc. on practically any type of substrate, even flexible ones [9], and allowing the tuning of the emission colour over the full visible spectrum. The techniques mentioned above, that do not require such complex equipments like those based in ultra high vacuum systems, have clearly contributed to increase the interest and the number of investigations in this field. Conducting polymers are usually employed as hole-transporting layer (HTL). *Poly(3,4-ethylenedioxythiophene)/poly(styrene sulfonate)*, (PEDOT:PSS) is the most commonly used in organic optoelectronic devices [10]. These conducting polymers are deposited from an aqueous dispersion by spin-coating method. Polyaniline (PANI) is another promising HTL for these kind of applications [11,12]. In doped form, PANI (emeraldine salt) is intrinsically conductive (4.4 Ω^{-1} cm^{-1}) [13]. Aqueous dispersions of PANI can be deposited by similar methods than PEDOT:PSS. Recently, water-dispersed *polyaniline:poly(styrene sulfonate)*, (PANI:PSS) has been used as hole injection layer in organic light-emitting diodes (OLEDs) [14]. Layer-by-layer films of *polyaniline* and *Ni-tetrasulfonated phthalocyanine*, (PANI/Ni-TS-Pc) have also been used for the same purpose in PLEDs [15].

A more attractive alternative is the direct electrochemical synthesis with simultaneous deposition of the polymer, from a solution containing the corresponding precursor monomer over the indium-tin oxide (ITO) substrate. Polymers prepared by this method have several advantages: Simple preparation method, good and tuneable conductivity [16], well controlled thickness [17], easy fabrication for large areas [18], patternable and uniform morphology and good adhesion to the electrode [19]. For example, thiophene-based conducting polymers have been electrodeposited from monomeric or oligomeric precursors for its application as HTLs in OLEDs, showing excellent properties [20-22].

Few studies can be found related to electrochemical synthesis of aniline-based conjugated polymers applied to this type of devices. Sulfonated polyaniline has been employed as HTL in an organic diode [23]. The performance obtained with the electrochemically synthesised layer is similar to that obtained with spin-coated PEDOT:PSS [24]. Electrochemically synthesised polyaniline doped with camphorsulfonic acid has been employed for a poly(3-hexythiophene)-based light-emitting diode [25] and also has been used as dispersant agent in a zinc-selenide quantum dot light emitting diode [26]. The layer of PANI is smooth and regular in all the cases, improving the electrical response of the device regarding the same devices in absence of this layer.

In this work we do an experimental study about the dependence of the electroluminescence of PVK-based devices, with different thicknesses of electrochemically deposited PANI buffer layers, on the excitation voltage.

2. Experimental

2.1. Devices fabrication

Five samples, each one with a different hole-transporting layer were fabricated. All devices fabricated had the same structural model: glass / ITO / Hole transporting layer / Active polymer / Al.

Poly(9-vinylcarbazole) (PVK) was employed as emissive active polymer for all devices and was purchased from Sigma-Aldrich. The five diodes possessed identical layers deposited under the same conditions with the exception of the hole transporting layer. It was inexistent in one case (A1 diode), in other one the widely known *Poly(3,4 ethylenedioxythiophene)/poly(styrenesulfonate)* (PEDOT:PSS) was used (A2 diode), and for the other three a electrochemically deposited layer of polyaniline, was employed in which the thickness was varied. Thus, A3 diode would be the one with the thickest layer of PANI, the intermediate would be A4 diode and finally A5 diode would be the thinnest.

Table 1 summarises the structure and the label assigned to each diode.

All devices studied in this work were fabricated starting with polished glass substrate coated with a thin (100 nm) semitransparent indium-tin oxide (ITO) layer of a resistivity of 60 Ohms cm which will act as the anode of the devices. These substrates were put under a cleaning procedure consisting in dipping the substrates in a NaOH 10% aqueous solution for three minutes at a temperature of 55 ºC. Then, they were rinsed with abundant deionized water for one minute approximately.

Table 1. Structure and label of all devices.

Label	Structure
A1	Glass/ITO/PVK/Al
A2	Glass/ITO/PEDOT:PSS/PVK/Al
A3	Glass/ITO/PANI-180nm/PVK/Al
A4	Glass/ITO/PANI-100nm/PVK/Al
A5	Glass/ITO/PANI-70nm/PVK/Al

For the A2 diode, a hole transporting layer was spin coated at a spin rate of 6,000 r.p.m. onto the ITO substrate reaching a thickness of about 75 nm from a 1.3 % PEDOT:PSS water solution -also supplied by Sigma-Aldrich for grade electronic applications-. Then, the layer was put under a hot plate curing process for 24 hours at 80 ºC in order to enhance the evaporation of the solvents. Only A2 diode contained this layer. For A3, A4 and A5 diodes, electrochemically deposited PANI was employed as a HTL. The thicknesses of each layer were varied as it is described below.

The chemicals used in this work were all reagent grade. Aniline was supplied by Merck and was distilled before use. The electrolytic medium employed in the voltammetric experiments was 0.50 M H_2SO_4 prepared with 18.2 MΩ cm resistivity water. The oxygen was initially purged from the electrochemical cells by bubbling a N_2 flow for 20 minutes, and the N_2 atmosphere was maintained during all the PANI depositions. ITO-covered glass substrates (60 Ohms cm) were used as working electrodes for the electrochemical synthesis-deposition of the conducting polymer. Previously to its use, ITO glass was degreased by sonication in an acetone bath and rinsed with abundant deionized water. The counter electrode was a platinum wire. An Ag/AgCl electrode was used as reference electrode (Crison), which was immersed in the working solution through a Luggin capillary.

The electrochemical synthesis of polyaniline was performed by potential cycling in a solution containing 0.10 M aniline. Fig. 1 shows a typical deposition experiment at a scan rate of 50 mV s^{-1}.

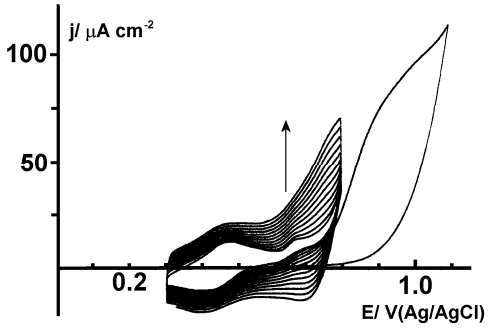

Fig. 1. Cyclic voltammograms of an ITO electrode immersed in a solution 0.10 M aniline + 0.50 M H_2SO_4. Scan rate 50 mV s^{-1}. Potential limits: 1st scan 0.3-1.1 V. 2nd and successive scans 0.3-0.8 V.

The polymer is oxidatively deposited at potentials above 0.75 V. In the first cycle, the potential was extended to + 1.1 V in order to promote nucleation sites for the electrochemical growth of the polymer. Then the rest of the deposition was performed by cycling between 0.3 and 0.8 V. The increase of the current during the successive cycles is indicative of the growth of the electroactive polyaniline on the ITO substrate. The thickness of the polyaniline layer depends on the number of cycles performed. The three different thicknesses were prepared by cycling 12, 24 and 50 times.

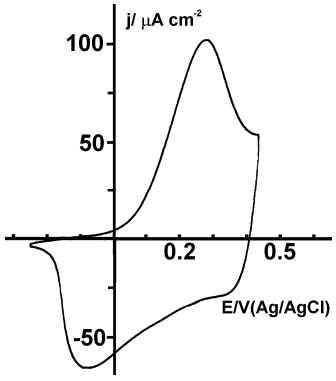

Fig. 2. Cyclic voltammograms of an ITO/PANI(24 cycles) electrode immersed in a solution 0.50 M H_2SO_4. Scan rate of 50 mV s^{-1}.

The resultant ITO/polyaniline electrode obtained was electrochemically characterized in an electrochemical cell containing aqueous H_2SO_4 in absence of monomer. Fig. 2 shows the typical electrochemical answer of a polyaniline layer synthesised in 24 potential cycles.

The redox transition from the reduced form (leucomeraldine) to the conducting form (emeraldine) is observed during the positive-going potential scan, with an oxidation peak centred at 0.28 V. This *p*-doping process is reversible and the dedoping process can be observed in the reverse scan with a reduction peak centred at - 0.08 V. The polyaniline film thickness can be estimated from the current density of the oxidation peak, as determined by Stilwell and Park [17]. The thickness of the layers measured from the electrochemical response was 70, 100 and 180 nm for the three samples prepared.

After the complete voltammetric characterization, the ITO/PANI electrodes were emersed from the electrochemical cell at a controlled potential of + 0.50 V, in order to preserve the conducting emeraldine doped form. Then the electrodes were rinsed and dried under a nitrogen flow for 24 hours prior to the fabrication of the devices.

Chemical structure of the polymers used as hole transporting layer can be observed at Fig. 3.

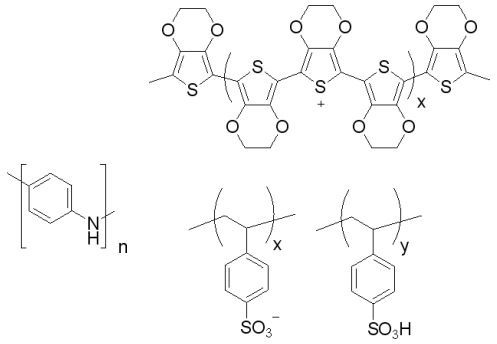

(a) (b)

Fig. 3. (a) Chemical structure of the polyaniline, used as hole transporting layer with three different thicknesses for A3, A4, A5 (b) Chemical structure of the PEDOT:PSS hole injector polymer, used by A2 diode.

For all diodes, a PVK active layer was spin cast from its 3% in weight toluene solution. The deposition conditions were a spin rate of 4,000 r.p.m. during 30 seconds. The thicknesses reached were about 60 nm. Fig. 4 shows the chemical structure of the polymer used as active layer of the performed devices.

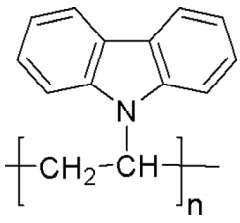

Fig. 4. *Chemical structure of the PVK polymer used as active layer for all diodes. The conditions of the deposition of this layer were identical regardless the hole transporting layer used.*

Finally, the metallization of the devices was carried out employing aluminium through mask using Joule effect method in a high vacuum chamber (10^{-7} mmHg). The thicknesses reached were about 600 nm.

All the performed diodes have circular shape with a size of 4 mm of diameter.

2.2. Methods

Optic and electronic characterization of all devices was carried out as well as the electrochemical characterization of the deposited PANI layers.

A Keithley 2400 Sourcemeter equipment was used to perform the electronic characterization, current versus voltage measure. With the aim to avoid the degradation of the polymeric samples, a pulsed voltage sweep was performed, in order to control de duty cycle. Fig. 5 shows the generic form of the mentioned pulsed waveform.

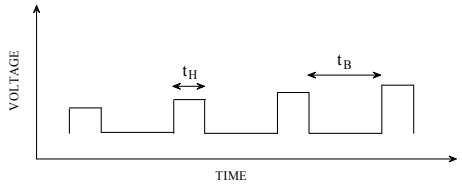

Fig. 5. Waveform of the Keithley 2400 Sourcemeter programmed pulsed employed in the electronic characterization (I-V) of the polymeric diodes (not on scale).

First of all, a study of the influence of the down time of the waveform in the electronic characterization was carried out. Concretely, measures for different down times (t_B); 20, 15, 5, 1, 0.5 and 0.1 seconds were performed, finding that it was not relevant to get the characterization curves for times above 0.1 s. Thus, one second for down-time (t_B) and seven milliseconds for up-time (t_H) were adopted to avoid degradation effects due to heat, being the duty cycle of the 0.7 % for all I-V curves presented in this paper.

The optical characterization of the devices is given by its electroluminescence curves. A Triax 190 monochromator and a multichannel thermoelectrically cooled CCD Symphony detector were employed to carry out the task. Both supplied by Horiba Jobin Yvon. The Keithley 2400 sourcemeter was also the responsible for the electric excitation of the diodes. For all electroluminescence measurements an integration time of five seconds was adopted.

3. Results and discussion

The aim of this study is to characterise the relation between the electroluminescence curves and the excitation voltage of each diode. In order to carry out this task, the electroluminescence of each diode was measured for different excitation voltages in a range from approximately 10 to 20 V. Electrochemically deposited PANI as the buffer layer was chosen for these diodes, in which the thicknesses of this layer were varied to study its dependence on the electroluminescence curves. To establish com-

parisons, PEDOT:PSS was also used as buffer layer in one case and no buffer layer was deposited in other.

It is well known that the energy emitted in each wavelength can be related to the electroluminescence curves by calculating the area under these curves. This can be done by integrating the electroluminescence curve between two given wavelengths. The result obtained will be proportional to the energy emitted by the diodes.

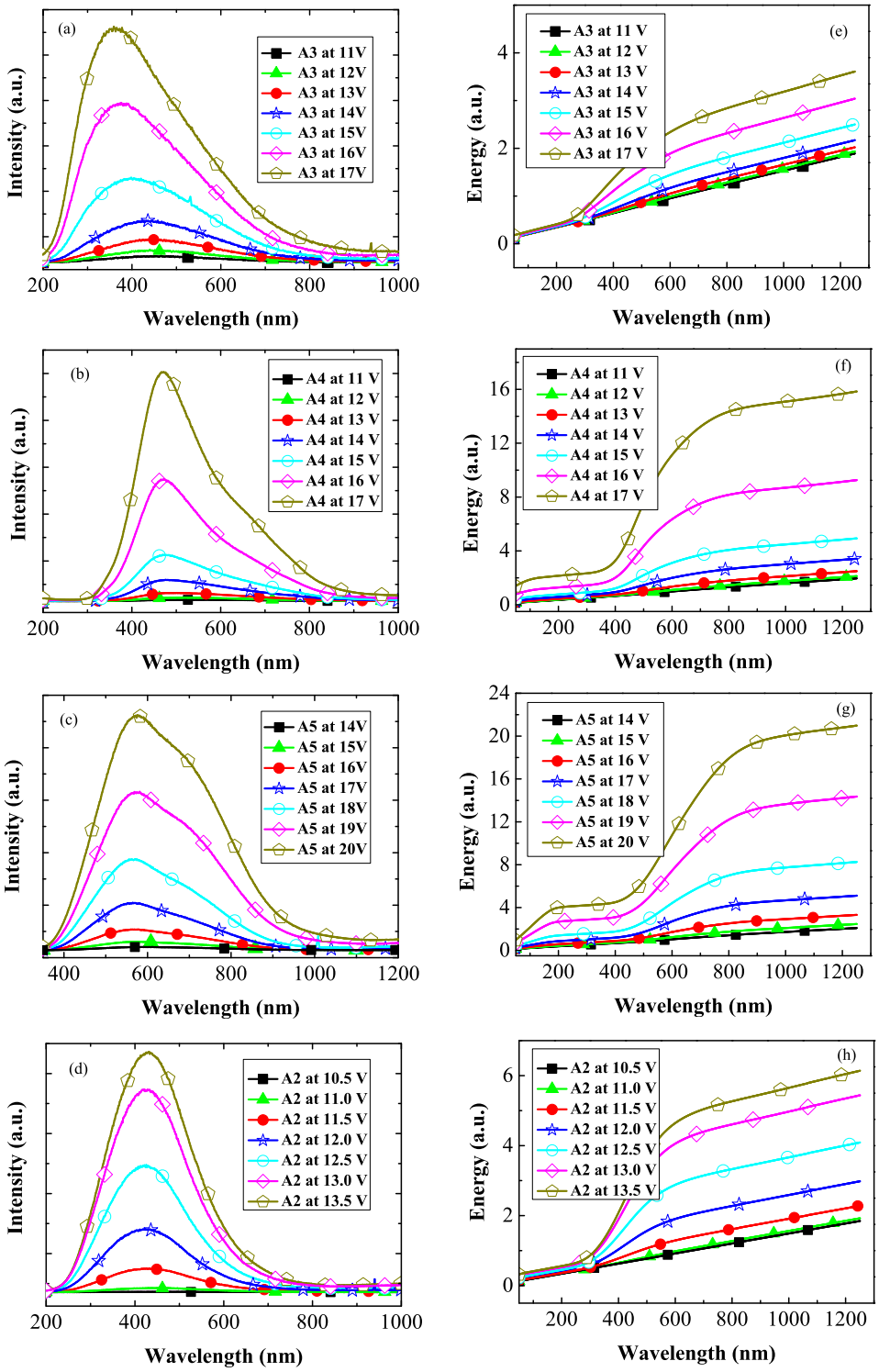

Fig. 6. Electroluminescence spectra for different excitation voltage values, and its corresponding integrated curves for each one of the excitation voltages applied. (a) A3 diode fabricated with a thick layer of PANI (180 nm). (b) A4 diode fabricated with an intermediate layer of PANI (100 nm). (c) A5 diode fabricated with a thin layer of PANI (70 nm). (d) A2 diode fabricated with a PEDOT:PSS buffer layer (75 nm). (e) Integrated curves corresponding to A3 diode. (f) Integrated curves corresponding to A4 diode. (g) Integrated curves corresponding to A5 diode. (h) Integrated curves corresponding to A2 diode.

In this way, the electroluminescence curves for each diode as a function of the excitation voltage, and its corresponding integrated curve are presented in Fig. 6. As it has been mentioned in previous sections, all devices followed the same fabrication process and laboratory conditions with the exception of the hole-transporting layer, in which different thicknesses were used: 70, 100 and 180 nm PANI layers, PEDOT:PSS, or simply no layer. Thus, any changes in electroluminescence and its corresponding integrated curves presented here should be attributed to the change in this buffer layer.

Figs. 6a to 6d show the electroluminescence curves of diodes A3 (PANI buffer layer of 180 nm), A4 (PANI buffer layer of 100 nm), A5 (PANI buffer layer of 70 nm) and A2 (PEDOT:PSS buffer layer of 75 nm). The corresponding integrated curves of the electroluminescence spectra for each one of the excitation voltages applied of figs 6a to 6d are displayed in Figs 6e to 6h. These curves must be interpreted as

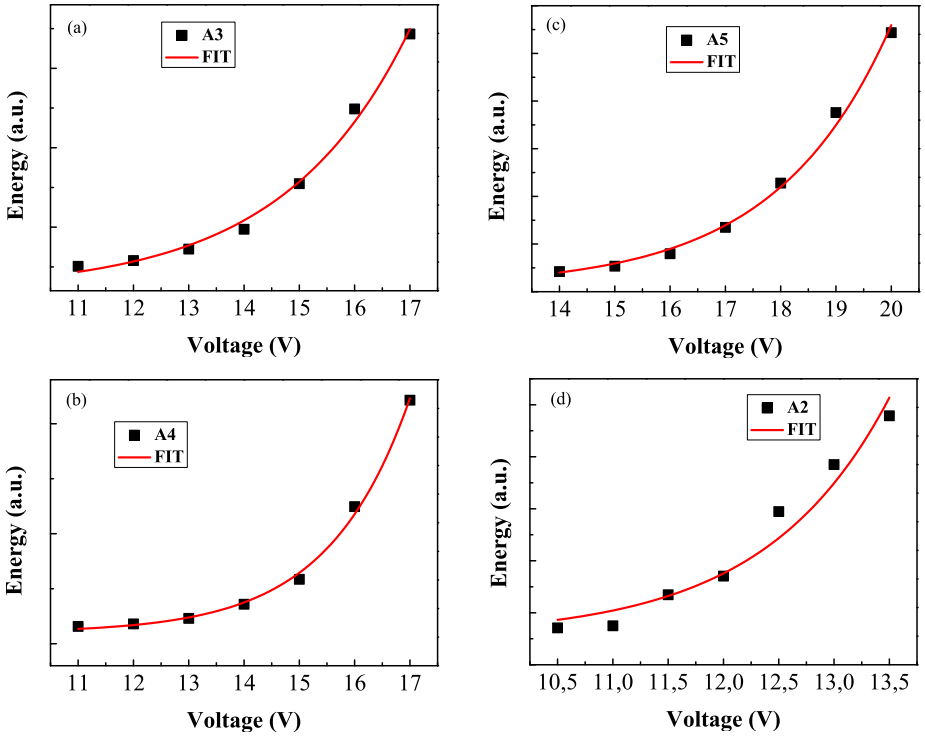

Fig. 7. Exponential growth least square fit of the Electroluminescence integrated curves as a function of the excitation voltage between anode and cathode of the devices. (a) Exponential fit corresponding to A3 diode. (b) Exponential fit corresponding to A4 diode. (c) Exponential fit corresponding to A5 diode. (d) Exponential fit corresponding to A2 diode.

accumulative curves. That is, each value of the curve for a given wavelength represents the area under its corresponding electroluminescence spectrum from 50 nm to the given wavelength. Thus, to calculate the energy emitted by the diodes, for example in the visible range, the ordinate energy value corresponding to 700 nm should be subtracted by that one corresponding to 400 nm.

In Figs 6e to 6h, it can be observed how the energy emitted by the diodes is higher as the excitation voltage is increased. It is obvious that this increase in energy emitted is not lineal because the enhancement experimented by changing the excitation voltage for example between 14 to 15 V is lower than that experimented between 18 to 19 V. This greater growth as the excitation voltage is increased suggests an exponential behaviour of the energy emitted by the diodes.

This exponential behaviour was demonstrated by performing an exponential growth least square fit of the electroluminescence integrated curves as a function of the excitation voltage between anode and cathode as can be observed at Figs. 7a to 7d. The square correlations coefficients obtained were in all the cases showed in Figs. 7a to 7d, greater than 0.9, which implies a very good exponential behaviour. Although it was not presented here, a variety of polynomical or power-type functions were assayed in order to find the better fit of the experimental data. For example, $y = a\, x^{b}$ power-type function was also used finding square correlations coefficients close to 0.9 but lower than those found in the exponential fit.

The experimental data of the Figs.7a to 7b were obtained from Figs. 6e to 6h respectively. In all the cases, the values of the energy fitted were taken from the area under the electroluminescence curves for different excitation voltages between 200 and 700 nm. Thus, each point at Figs. 7a to 7b represents the energy emitted among the wavelengths comprised between 200 to 700 nm. The same exponential behaviour was obtained for other range of wavelengths.

The spectra and the corresponding integrated curves of the A1 diode (no hole transporting layer was deposited, the active polymer was cast directly onto the ITO-covered-glass substrate) were also carried out. Nevertheless, no exponential behaviour was found. In fact, by increasing the excitation voltage not always an increase of the energy emitted was achieved. Furthermore, the obtained spectra were too noisy, and the devices degraded rapidly. This could be attributed to the lack of any buffer layer, since this layer is the responsible for decreasing the barrier at the interface of the ITO electrode and the active polymer -PVK in this case- and ensure the hole injection. The highest occupied molecular orbital (HOMO) and the lowest unoccupied molecular orbital (LUMO) are 5.8 eV and 2.3 eV for the PVK active polymer, respectively, whereas the Fermi level of the ITO electrode is around 4.8 eV. Thus, the barrier height between the ITO electrode and the emissive polymer is around 1 eV, and consequently, a large barrier for injection of holes from ITO electrode, which translates into a low luminance and a high onset voltage. In this context it is relevant to introduce any buffer layer that helps to reduce the mismatch between the anode work function and the HOMO level of the emissive polymer. Table 2 summarises the exponential fit results obtained in this section.

Table 2. Coefficients of the Exponential Least-square fit results: y = C1 Exp (x / C2) + C3

Diode	C1 (a.u.)	C2 (V)	C3 (a.u.)10^5	CORR. (R^2)
A3	1000	2.28	6.00	0.993
A4	100	1.47	4.97	0.997
A5	730	2.08	1.92	0.995
A2	30	1.13	5.42	0.959

The most relevant data in Table 2 are the square correlation coefficient (last column), that indicates which exponential behaviour is better, and the C2 coefficient inside the exponential (third column), which has voltage units and indicates how fast the exponential growth is.

From the point of view of the square correlation coefficient, the worse fit was found for the A2 diode (PEDOT:PSS buffer layer), although it was larger than 0.9 showing a very good exponential behaviour. The rest of the diodes, employing electrochemically deposited PANI buffer layer were better fitted, but no relation was found between the thickness of the PANI layers and the correlation coefficient. That is, by increasing PANI thickness, no better fit was achieved.

However, attending the electronic characterization of the devices -current versus voltage curves-, a determined tendency was observed in terms of the onset voltage of the diodes. This implies that the observed tendency could be due to the hole transporting layer deposited in each case. Thus, A3 diode that uses the PANI-180 layer presents a better performance from the point of view of the turn-on voltage, that is, a lower voltage is needed to reach the same current levels than the other diodes. In fact, A3 diode presents an even better performance than A2 diode, which contains the widely used PEDOT:PSS layer. On the third place is the A4 diode that has the PANI-100 layer, but followed very close by the A5 diode that has the PANI-70 layer, because the difference in thickness between these diodes is smaller than the one existing between them and the A3 diode. Finally, the worst behaviour is found for the A1 diode which has no hole transporting layer. This corroborates the mentioned tendency since A1 diode could be considered as one with a zero thickness buffer layer. Fig. 8 shows this behaviour.

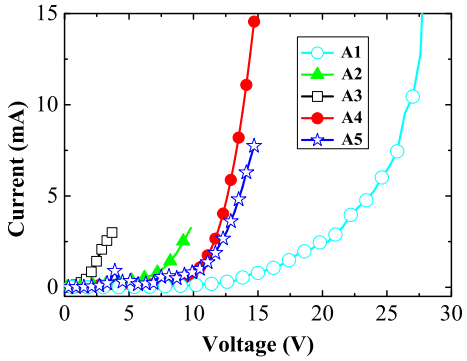

Fig. 8. Current versus voltage curves of diodes using the conjugate polymer PVK as active layer. A decrease of the turn-on voltage as a function of the hole transporting layer and the thickness for each diode is observed.

This experimental fact confirms that the polymer employed as hole transporting layer and its thickness is determinant in the shape of the I-V characteristic and concretely in the turn-on voltage of these curves. This factor suggests that by means of electrochemical deposition of a PANI hole transporting layer, a rigorous control of the thickness can be achieved, being an easy way of fabrication. Therefore the designer might be able to do the tuning of the turn-on voltage of the I-V characteristic. The obtained results are in consonance with those found in the bibliography [14,15,25,27,28].

On the other hand, it is generally interesting to have a low driving voltage attending to power consumption and depending on the application. This can be achieved employing a PANI hole transporting layer of about 180 nm instead of the so used PEDOT:PSS layer with typical thickness.

Putting together the curves of electroluminescence of Figs. 6a to 6d -only one curve of each figure with the same excitation voltage-, a shift with the wavelength is observed depending on the buffer layer and the thickness –as PANI is concern- employed for each diode. Nevertheless, the spectra are quite broad, overlapping a great part of them. Similar results were explained by Leger et al. [29] using multilayer optics. The normalised spectra are presented in Fig. 9. No treatment of the experimental data was done, with the exception of the background removing and the smoothed of the A1-diode curve –because it was too noisy-.

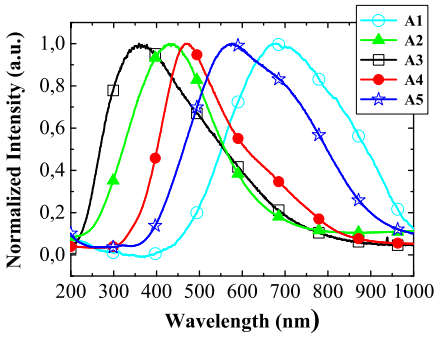

Fig. 9. Electroluminescence normalized spectra of the diodes (PVK as active layer). The excitation voltage has been the same for all diodes. An emission maximum shift has been observed for each diode as a function of the type and the thickness of buffer layer deposited.

Thus, the emission maximum of the A3 diode, fabricated with the PANI-180 layer would be about 60 nm below the one fabricated with PEDOT:PSS (A2), whose electroluminescence maximum is about 430 nm. The next peak is that of A4 (PANI-100), and following shortly is the diode fabricated with the PANI-70 layer (A5). Finally, the maximum of the A1 diode which has no buffer layer is found at larger wavelengths.

Remarkably, the order followed by the curves of Fig. 9 advancing in wavelengths is the same followed by I-V curves of Fig. 8 advancing in voltage. That is, first, the emission curve of the diode that has been fabricated with the thicker PANI layer is found. That fabricated with PEDOT:PSS as transporting layer is found next, followed by the intermediate and the thinnest PANI layer. Finally, the curve of the device that has no buffer layer is found at longer wavelengths.

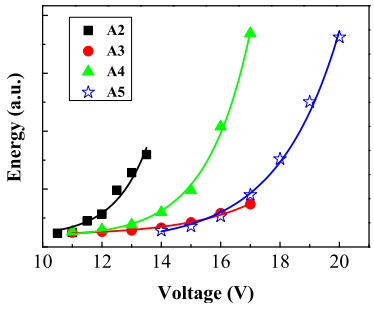

Fig. 10. *Exponential growth least square fit of the Electroluminescence integrated curves putted together as a function of the excitation voltage between anode and cathode of the devices.*

In this context, with the aim to investigate whether the fitted curves (7a to 7d) are arranged in the same manner, they have been put together in Fig. 10. No such behaviour is observed, because the way in which the fitted curves grow is not related to the thickness of the PANI or the type of buffer layer employed for each diode. On the contrary, as it could not be otherwise, the order followed by these curves is tightly related to the C2 coefficient (third column in Table 2). Hence, the smaller is the C2 coefficient the faster is the exponential growth, but no correlation exists with the type or the thickness of the buffer layer used.

4. Conclusions

Five polymeric samples using PVK as emission layer have been prepared. The buffer layer of the devices was varied. In one case, no such layer was deposited, in other one, the commonly used PEDOT:PSS polymer was deposited by spin-coating (75 nm), and for the rest of the diodes an electrochemically deposited PANI layer was employed, generating three different thicknesses: 180, 100 and 70 nm.

Fitting the integrated curves of electroluminescence from 200 to 700 nm as a function of the excitation voltage, a very good exponential behaviour has been demonstrated. The square correlation coefficients were all greater than 0.9, with the exception of the diode A1 -which had no buffer layer- inasmuch no exponential behaviour was found. This fact was attributed to the lack of any buffer layer since it is the responsible for ensuring the hole injection by decreasing the barrier height between the ITO electrode and the HOMO level of active polymer.

The samples in which electrochemically PANI had been deposited presented better square correlation coefficients than those using PEDOT:PSS, being all greater than 0.99.

A lower turn-on voltage has been found for devices using thicker PANI buffer layers, whereas a shift in the electroluminescence spectra has been observed. Furthermore, the order followed by the spectra curves advancing in wavelengths is the same followed by I-V curves advancing in voltage. That is, first, the emission curve of the diode that had been fabricated with the thicker PANI layer, secondly that fabricated with PEDOT:PSS as transporting layer, followed by the intermediate and the thinnest PANI layer. Finally, the curve of the device that had no buffer layer was found at longer wavelengths.

On the contrary, joining all the exponential least square fits no such tendency was found. So, there is no relation between how fast the exponential grows and the type or the thicker of the buffer layer employed.

Acknowledgments

This work has been partially supported by grants UMH-Bancaja 2007; GV/2007/32 Consellería de Empresa, Universidad y Ciencia (Generalitat Valenciana), projects MAT2006-04057 (Spanish Ministry for Education and Science) and FEDER. Authors thanks Dr. F. Montilla and Dra. M. A. Cotarelo for the electrochemical synthesis of the polyaniline. PLEDs were metallized in the IMB-CNM-CSIC under program GICSERV: GIC-16-1-2006 and GIC-27-1-2007. The contacts of the devices have been realized at the Institute for Systems based on Optoelectronics and Microtechnology (ISOM) under "Large-Scale Scientific and Technological Facilities (ICTS)" program from Spanish Ministry for Education and Science (ICTS-2006-01)

References

[1] J. H. Burroughes, D. D. C. Bradley, A. R. Brown, R. N. Marks, K. Mackay, R. H. Friend, P. L. Burns, A. B. Holmes, Nature **347**, 539 (1990)

[2] D. Braun, A. J. Heeger, Appl. Phys. Lett. **58**, 1982 (1991)

[3] D. Braun, A. J. Heeger, H. Kroemer, J. Electron. Mater. **20**, 945 (1991)

[4] S. R. Forrest, Org. Electron. **4**, 45 (2003)

[5] H. Spanggaard, F. C. Krebs, Sol. Energy Mater. Sol. Cells **83**, 125 (2004)

[6] P. Schilinsky, C. Waldauf, J. Hauch, C. J. Brabec, Thin Solid Films **451**, 105 (2004)

[7] S. A. McDonald, G. Konstantatos, S. Zhang, P. W. Cyr, E. J. D. Klem, L. Levina, E. H. Sargent, Nat. Mater. **4**, 138 (2005)

[8] J. L. Alonso, J. C. Ferrer, R. Mallavia, S. Fernández De Ávila, J. Optoelectron. Adv. Mater. **10**, 169 (2008)

[9] G. Gustafsson, Y. Cao, G. M. Tracy, F. Klavetter, N. Colaneri, A. J. Heeger, Nature **357**, 477 (1992)

[10] Y. Cao, G. Yu, C. Zhang, R. Menon, A. J. Heeger, Synth. Met. **87**, 171 (1997)

[11] C. Tengstedt, A. Crispin, C. H. Hsu, C. Zhang, I. D. Parker, W. R. Salaneck, M. Fahman, Org. Electron. **6**, 21 (2005).

[12] M. Boubaya, M. A. Belhadj, H. Zangar, G. Blaise, J. Phys. D-Appl. Phys **40**, 4297 (2007)

[13] J. Stejskal, R. G. Gilbert, Pure Appl. Chem. **74**, 857 (2002)

[14] J. Jang, J. Ha, K. Kim, Thin Solid Films (2007), doi:10.1016/j.tsf.2007.08.088.

[15] J. C. B. Santos, L. G. Paterno, E. A. T. Dirani, F. J. Fonseca, A. M. de Andrade, Thin Solid Films (2007), doi:10.1016/j.tsf.2007.08.140.

[16] K. Gurunathan, A. V. Murugan, R. Marimuthu, U. P. Mulik, D. P. Amalnerkar, Mater. Chem. Phys. **61**, 173 (1999)

[17] D. E. Stilwell, S. M. Park, J. Electrochem. Soc. **135**, 2491 (1988)

[18] G. W. Jang, C. C. Chen, R. W. Gumbs, Y. Wei, J. M. Yeh, J. Electrochem. Soc. **143**, 2591 (1996)

[19] F. Brovelli, J. C. Bernede, S. Marsillac, F. R. Diaz, M. A. del Valle, C. Beaudouin, J. Appl. Polym. Sci. **86**, 1128 (2002)

[20] H. Q. Tang, Z. X. Zhou, Y. B. Zhong, H. X. Liao, L. H. Zhu, Thin Solid Films **515**, 2447 (2006)

[21] G. M. Wang, X. Hu, T. K. S. Wong, Appl. Surf. Sci. **174**, 185 (2001)

[22] G. M. Wang, X. Hu, T. K. S. Wong, J. Solid State electrochem. **5**, 150 (2001)

[23] L. S. Roman, R. M. Q. Mello, F. Cunha, I. A. Hum melgen, J. Solid State electrochem. **8**, 118 (2004)

[24] A. R. V. Benvenho, J. P. M. Serbena, R. Lessmann, I. A. Hummelgen, R. M. Q. Mello, R. W. C. Li, J. H. Cuvero, J. Gruber, Braz. J. Phys. **35**, 1016 (2005)

[25] J. S. Kim, S. K. Kim, H. B. Gu, Mol. Cryst. Liquid Cryst. **405**, 113 (2003)

[26] D. Kaushik, M. Sharma, R. R. Singh, D. K. Gupta, R. K. Pandey, Mater. Lett. **60**, 2994 (2006)

[27] Y. Yang, A. J. Heeger, Appl. Phys. Lett. **64**, 1245 (1994)

[28] Y. Yang, E. Westerweele, C. Zhang, P. Smith, A. J. Heeger, J. Appl. Phys. **77**, 694 (1995)

[29] J. M. Leger, S. A. Carter, B. Ruhstaller, H. –G. Not hofer, U. Scherf, H. Tillman, H. –H. Hörholf, Phys. Rev. B **68** 54209 (2003)

*Corresponding author: j.l.alonso@umh.es